International Journal of Fluid Machinery and Systems
Vol. 2, No. 4, October-December 2009

Original Paper

A New Blade Profile for Bidirectional Flow Properly Applicable to a Two-stage Jet Fan

Michihiro Nishi[1], Shuhong Liu[2], Kouichi Yoshida[1], Minoru Okamoto[3] and Hiroyasu Nakayama[4]

[1]Department of Mechanical Engineering, Kyushu Institute of Technology
1-1 Sensui-cho, Tobata, Kitakyushu, 804-8550, Japan
[2]Department of Thermal Engineering, Tsinghua University
Beijing, 100084, China
[3]Department of Human Life, Kyushu Women's University
1-1, Jiyugaoka, Yahata-nishi, Kitakyushu, 807-8586, Japan
[4]Department of Mechanical Engineering, Kitakyushu National College of Technology
5-20-1, Shii, Kokura-minami, Kitakyushu, 802-0985, Japan

Abstract

A reversible axial flow fan called jet fan has been widely used for longitudinal ventilation in road tunnels to secure a safe and comfortable environment cost-effectively. As shifting the flow direction is usually made by only switching the rotational direction of an electric motor due to heavy duty, rotor blades having identical aerodynamic performance for bidirectional flow should be necessary. However, such aerodynamically desirable blades haven't been developed sufficiently, since most of the related studies have been done from the viewpoint of unidirectional flow. In the present paper, we demonstrate a method to profile the blade section suitable for bidirectional flow, which is validated by studying the aerodynamic performances of rotor blades of a two-stage jet fan experimentally and numerically.

Keywords: Blade profile, Wall curvature, Bidirectional flow, Jet fan, Aerodynamic performance, Turbulent flow analysis

1. Introduction

A reversible axial flow fan called jet fan has been widely used for longitudinal ventilation in road tunnels to secure a safe and comfortable environment cost-effectively. Various researches and developments of jet fan have been made, and it is said that the fan has the satisfactory performance for the present needs. However, if the future need is concerned, it is still necessary to develop a jet fan having higher aerodynamic performance, for efficient usage of energy in every engineering system is vital in the low carbon society.

From the aerodynamic view, a cambered airfoil is regarded as favorable for the rotor (or impeller) blade like a unidirectional axial fan and the variable pitch mechanism is used to set the blade oppositely if the flow direction should be reversed in case of emergency. But, owing to very heavy duty as a safety measure, a reversible fan without this kind of mechanism has been adopted in actual cases. That is, such a method to drive the rotor in the reverse direction is used for switching the flow direction. As the fan should provide almost the same performance in both flow directions, those symmetrical blades without camber are used in the case of single stage fan rotor. The other structure is a 2-stage jet fan where two rotors are assembled to both sides of motor shaft. If higher speed jet from the fan is expected, the latter will be preferable. Though there are vast amounts of studies treating airfoil sections (e.g.: Abbot and von Doenhoff [1]), most of them have been done from the viewpoint of unidirectional flow. Thus, aerodynamically desirable airfoil sections for bidirectional flow are still regarded as unresolved.

As one of the typical sections is a symmetrical circular-arc airfoil, this section has been actually used for the rotor blade of a jet fan (Nishioka, et al.[2]). Generally, airflow easily separates from the leading edge at a certain angle of attack for a blade having the sharp edge. However, it is known that aerodynamic performance of the blade doesn't deteriorate, once the separating flow reattaches the blade surface downstream. This knowledge indicates that the key to secure the performance is attributed to the stable reattachment of the separating flow on the surface. From this view, the wall surface consisting of concave and convex curves shown in Fig. 1 is taken up for consideration. Though it will be nice if this profile is usable for the blade in bidirectional flow, stable reattachment of separating flow shown in Fig. 1 is really accomplished in actual flow cases. Thus, we have investigated the capability of the proposed blade profile for bidirectional flow by using a two-stage jet fan experimentally and

Received September 11 2009; accepted for publication October 26 2009: Review conducted by Dr. Shogo Nakamura. (Paper number O09041)
Corresponding author: Michihiro Nishi, Professor Emeritus, nishi_michihiro@yahoo.co.jp

numerically in the present study.

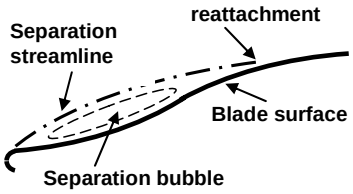

Fig. 1 Reattachment of separating flow to the blade surface

2. Test Blade

For validation of the present idea, the most reliable approach will be the direct performance test of the jet fan that has the proposed rotor blades. As we have been conducted experimental studies using JF600 models (Tukamoto, et al.[3], Nishi, et al.[4]), the following two kinds of rotor blades for JF600 are prepared in this study:

Blade C: conventional symmetrical airfoil similar to NACA0010, which is basically used for unidirectional flow. Chord length = 150 mm, AR = 1.0, σ_{tip} = 0.62, σ_{root} = 1.19

Blade D: new symmetrical airfoil based on the present idea (foil surface having negative and positive curvatures) Chord length = 170 mm, AR = 0.9, σ_{tip} = 0.70, σ_{root} = 1.35

Five blade sections (stream surface: root, ¼, ½, ¾, and tip) are stacked for both blades and are shown in Fig. 2, where variation of stagger angle with respect to radial position is determined to satisfy the conditions below:

Inner diameter of cylindrical casing = 630 mm
Tip clearance ratio = 0.64%
Discharge = 9.35 m^3/min at rotational speed less than 2200 rpm
Constant chord and thickness of 10%
Number of rotor blades = 8
Flow pattern (Vortex type) at the front blade exit:

$$V_u = const. \quad (1)$$

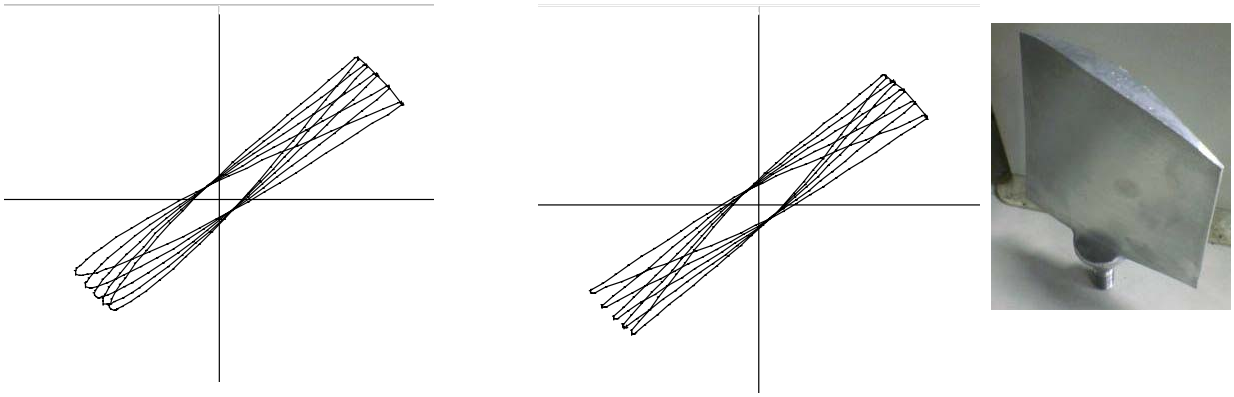

(a) Blade C (b) Blade D

Fig. 2 Cross section of rotor blades

3. Experimental Apparatus and Method

3.1 Test Jet Fan and Measurement System

Cross sectional view of the test 2-stage jet fan [4] and the measurement system are schematically shown in Fig. 3. It is noted that the axial length of cylindrical casing with silencer is 0.4 m shorter than that of standard jet fan, usually called as JF-600. The test fan is hung on the beam attached to the frame construction. Each of two rotors is mounted on the shaft of an electric motor of 11kW, rotational speed of which is variable between 0 rpm and 2300 rpm by an inverter controller. The motor is supported with three struts of flat plate equally spaced in the cylindrical casing. The setting angle θ of rotor blade is adjustable so as to study its effect on the fan performance.

The flow measurement device is such that eight three-hole Pitot tubes mounted on the rotatable support in the peripheral direction and they are arranged in the radial positions following the Japan Industrial Standard (JIS) for flow-rate measurement, as shown in Fig. 4. This is set at the fan exit to measure pressure P and velocity V near the silencer outlet (represented by S6 section), for variations of them cannot be regarded as negligible.

To investigate the flow field in the casing, a five-hole Pitot tube was traversed in the radial direction at five sections. As S2 and S5 are regarded as the inlet of first stage and the outlet of second stage respectively, the measured data are used to calculate the aerodynamic performance of the fan. Noise measurement was also made at the exit side following the JIS.

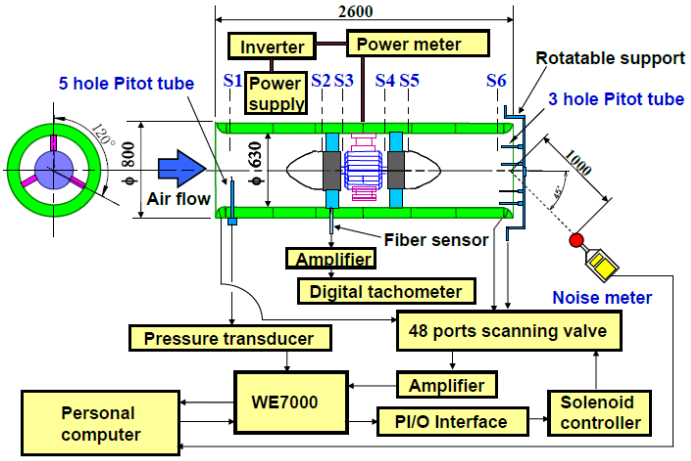

Fig. 3 Test jet fan and measurement system

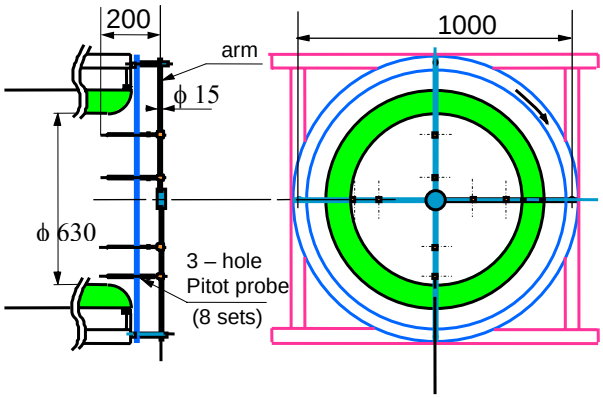

Fig. 4 Flow measurement device at the exit

3.2 Parameters

If radial component of velocity is disregarded, axial component of velocity V_{z6} at S6 section is calculated from

$$V_{z6} = V_6 \cos\beta_6 \tag{2}$$

where β denotes flow angle from the axial direction.

Flow rate is calculated from equation (3), where A_j denotes the cross sectional area of cylindrical casing.

$$Q = \int_{A_j} V_{z6}\, dA \tag{3}$$

The number of jet fans installed in a road tunnel is usually decided considering the axial thrust generated by those fans, as the wall friction loss due to the tunnel stream for ventilation is approximately balanced with the longitudinal force provided by the fans. Thus, measurement of the thrust at the performance test should be mandatory. Assuming that a complete jet fan unit tested in the still air condition is regarded as standard, the axial thrust F is measured by using the indirect method [3], which is given by

$$F = \rho\int_{A_j} (V_{z6}^{\,2} - V_{z1}^{\,2})\, dA + \int_{A_j} (P_6 - P_1)\, dA + \int_{A_B} (P_{B6} - P_{B1})\, dA_B \tag{4}$$

where $dA_B = dA\cos\gamma$

A_B : projected area of casing lip normal to z direction

γ : an angle of inclination of casing wall from r direction

P_B : pressure acting on the casing lip

It is noted that the ideal value F_0 given by equation (5) is used as its index, which is known to overestimate the actual axial thrust of jet fan.

$$F_0 = \rho Q^2 / A_j \tag{5}$$

Since S2 and S5 represent the inlet and the exit of 2-stage axial fan respectively, the total pressure rise P_T is specified as an increase in total pressure between S2 and S5 sections, following the standard test codes for fans. Consequently, the fan total efficiency η is expressed as

$$\eta = \frac{QP_T}{L} = \frac{Q(\overline{P}_{t5} - \overline{P}_{t2})}{L} \tag{6}$$

where $\overline{P}_t = \int P_t V_z\, dA \,/\, \int V_z\, dA$ and L denotes the shaft power.

To evaluate the fan noise, specific noise level given by the following equation is used.

$$SPL_{SA} = SPL_A - 10\log(Q\,P_T^{\,2}) + 2 \tag{7}$$

where SPL_A denotes the sound pressure level (A-characteristic).

4. Results and Discussion

4.1 Experimental Performance

As the measurement of axial thrust is inevitable at the performance test, a complete unit should be used for the test. In this case, the aerodynamic performances can only be obtained at a single operating point. Thus, the rotational speed n (rpm) and the setting angle of blade θ (θ=0: design stagger angle, and θ>0: decrease in stagger angle) are selected as experimental parameters in this study. Test range of the former was between 1600 rpm and 2200 rpm, and that of the latter was between -5 deg and 5 deg.

4.1.1 Flow rate and axial thrust

Variation of flow rate Q (m^3/min) and that of axial thrust F (N) against the rotational speed n (rpm) are shown in Fig. 5 and Fig. 6 respectively for two jet fans, one of which has Blade C and the other of which has Blade D. Almost the same results are observed. That is, the difference between Blade C and Blade D is quite slight, but both Q and F for Blade D are a little bit larger

than those of Blade C. And steady flow is observed at every operating point in the test range. Thus, it is suspected that the idea shown in Fig. 1 is almost actualized. This favorable result may be attributed to not only the blade profile but the following flow mechanism: As the secondary flow from the root to the tip along the blade surface occurs due to blade rotation, it sweeps the low energy flow in the separated zone and flow reattachment is almost always attained.

From the linear relationship between n and Q, the similarity law is valid in the present test range, where the blade load is possible to increase with the increase of setting angle. It is seen that both rotor blades are usable from the Japanese guideline of 480 m^3/min if rotational speed and the setting angle are properly selected.

Consequently, we can realize that the present method for profiling the blade section of jet fan rotor has worked satisfactory.

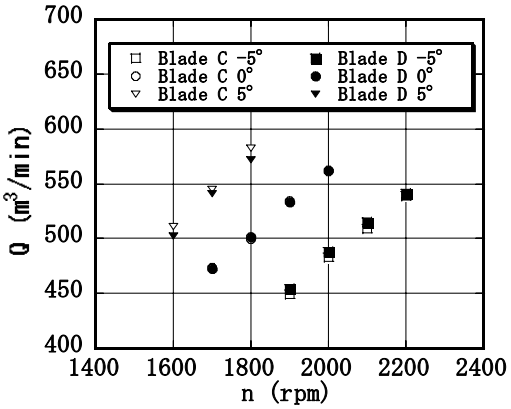

Fig. 5 Variation of flow rate against rotational speed

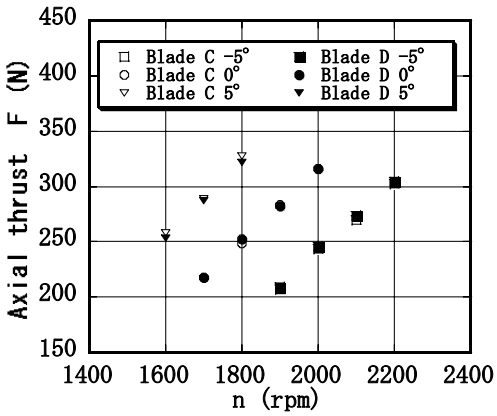

Fig. 6 Variation of axial thrust against rotational speed

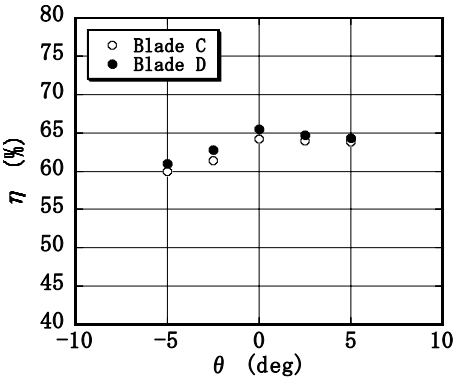

Fig. 7 Fan efficiency vs. blade setting angle

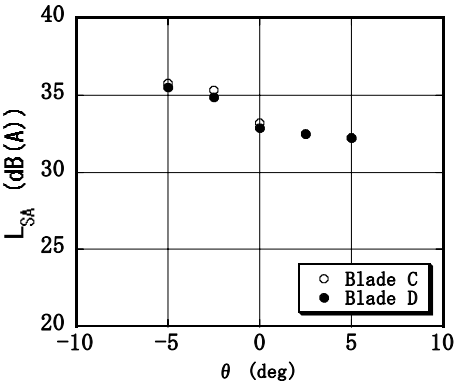

Fig. 8 SPL_{SA} (= L_{SA}) vs. blade setting angle

4.1.2 Efficiency and noise level

Regarding fan efficiency and specific noise level, they are plotted against the setting angle θ in Fig. 7 and Fig. 8. Similar to flow rate and axial thrust, both results for Blade D are a little bit larger than those for Blade C. The maximum efficiency of 65% is obtained at the design condition (θ = 0 deg). The efficiency is nearly constant in the range of positive setting angle up to 5 deg, but it varies with the angle in the negative range.

Regarding the noise level, SPL_{SA} gradually decreases with the increase the setting angle in the present test range. And the minimum value around 32 dB(A) is observed at θ = 5 deg. From the examination that the sound decay with distance is satisfactorily represented by the following equation, SPL_A at the location of 1.5 m is suspected to reach 30 dB(A).

$$\Delta SPL_A = 20 \log \frac{I_0}{I} \qquad (8)$$

where I_0: distance from noise source to the standard location I: distance from the source to measurement location.

As slight decrease is achieved if Blade D is used instead of Blade C, frequencies of the fan noise are investigated by using the one-third octave-band. A typical result is shown in Fig. 9, where the noise component of 1600 Hz and the broad band noise are predominant. Two other dominant components are 267 Hz and 800 Hz. The frequency of 1600 Hz corresponds to 2 $Z_r Z_s$ (n / 60) = 2 x 8 x 3 x (2000/60), where Z_r and Z_s are the number of rotor blades and struts respectively.

4.2 Internal Flow

Radial distributions of velocities V_z and V_u at two locations, S3 for the front rotor exit and S5 for the rear rotor exit are shown in Fig. 10, where each velocity is normalized by the peripheral velocity at blade tip U_t.

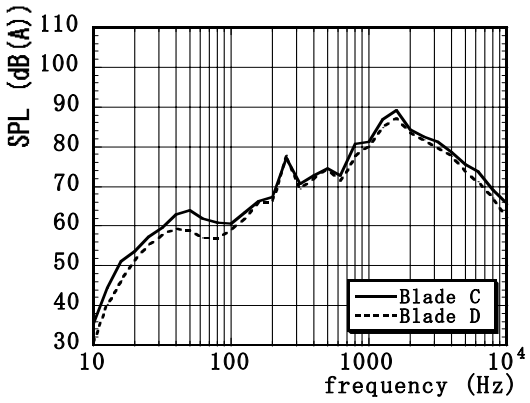

Fig. 9 1/3 octave band analysis of fan noise

They were measured by traversing a five-hole Pitot tube in the radial direction from the casing wall. The following features of flow are observed:

(a) S3 section (front rotor exit):

Axial velocity is nearly uniform in the center region, but its deficit near the casing wall and hub wall cannot be treated negligible.

Circumferential velocity is almost regarded as constant, which reasonably corresponds to the present design vortex type.

(b) S5 section (rear rotor exit):

The uniform zone of axial velocity decreased by comparison with that at S3.

As the rear rotor also works, the circumferential velocity is larger than that at S3.

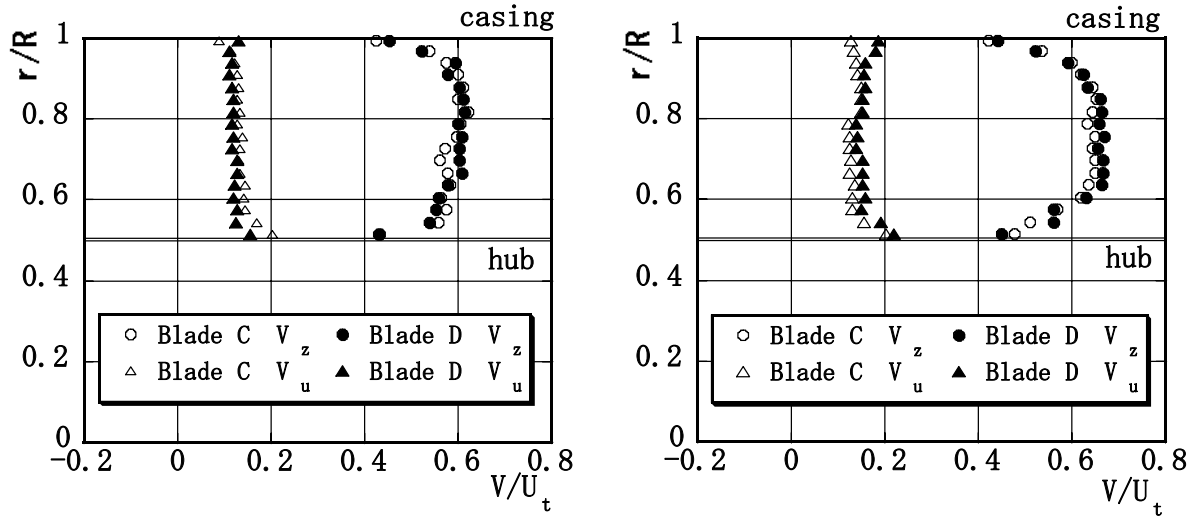

(a) measurement made at S3 section (b) measurement made at S5 section

Fig. 10 Radial distributions of velocity (θ = 0 deg, n = 2000 rpm)

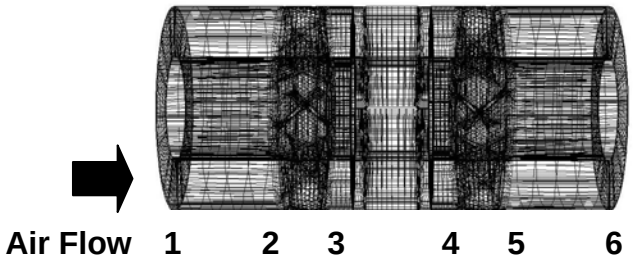

Fig. 11 Computational domain (Grids: 737919)

4.3 Numerical Simulation for Consideration

To deepen our understanding of those test results, the steady turbulent flow analysis based on the continuity equation and RANS equations was conducted by using the commercial CFD software CFX-TASCflow with k-ω turbulence model. As shown in Fig. 11, the computational domain is set between S1 and S6 sections of jet fan so that it is a cylindrical annular pipe where two rotors and the strut between the front rotor and the rear are installed. The axsymmetric uniform velocity is assumed at the inflow plane and a mass flow is set at the outflow plane as the boundary conditions.

4.3.1 Validation

As the simpler domain is treated in the present simulation, computational results of internal flow are at first evaluated by comparison with the experimental data measured by a five-hole probe. One of examples is shown in Fig. 12, where velocity distributions at the exits of two rotors with Blade C are arranged. We can recognize the reasonable correspondence between the experiments and the numerical simulations, though the difference between them is observed in the zone near the casing wall. It is suspected that the assumption of uniform flow at the inflow plane is one of major causes.

4.3.2 Performance prediction

Using the present simulation model, performance prediction is attempted. Table 1 shows the results. The following features are deduced:

(1) Better aerodynamic performance of Blade D than that of Blade C is predicted.

(2) The measurement result is qualitatively explained by the steady flow simulation.

(3) Total pressure rise done by the front rotor doesn't differ too much between Blade C and Blade D, but the rise by the rear rotor of Blade C is much smaller than that of Blade D. Same trend is observed in efficiency.

(4) This is understandable because the geometry of Blade B is decided based on the unidirectional flow so it doesn't provide a good performance in the case of the counter flow.

4.3.3 Blade wake

As the broad band noise was one of major causes for the fan noise from Fig. 9, distributions of turbulence kinetic energy just downstream of the rear rotor blade are correlated numerically and plotted by using a contour map in Fig. 13 (a) and (b). The former is for Blade C and the latter corresponds to Blade D. The wake region of Blade C is greater than that of Blade D so that it is realized that the broad band noise is primarily related to the blade wake.

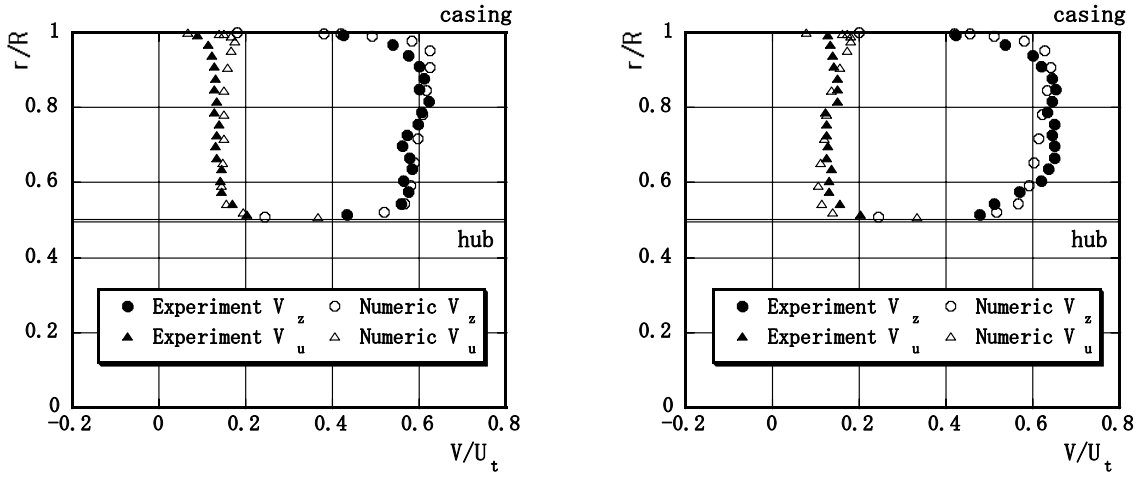

(a) velocity distributions at S3 section (b) velocity distributions at S5 section

Fig. 12 Comparison of simulation with experiment (θ = 0 deg, n = 2000 rpm)

Table 1 Prediction of aerodynamic performance

n = 2000 rpm		power (kW)	ΔP (Pa)	η (%)
Blade C	front rotor	5.06	446	80.7
	strut	-	- 50	-
	rear rotor	1.6	93	53.2
	2 stage	6.65	489	67.2
Blade D	front rotor	5.25	458	79.7
	strut	-	- 55	-
	rear rotor	2.41	194	73.6
	2 stage	7.66	597	71.2

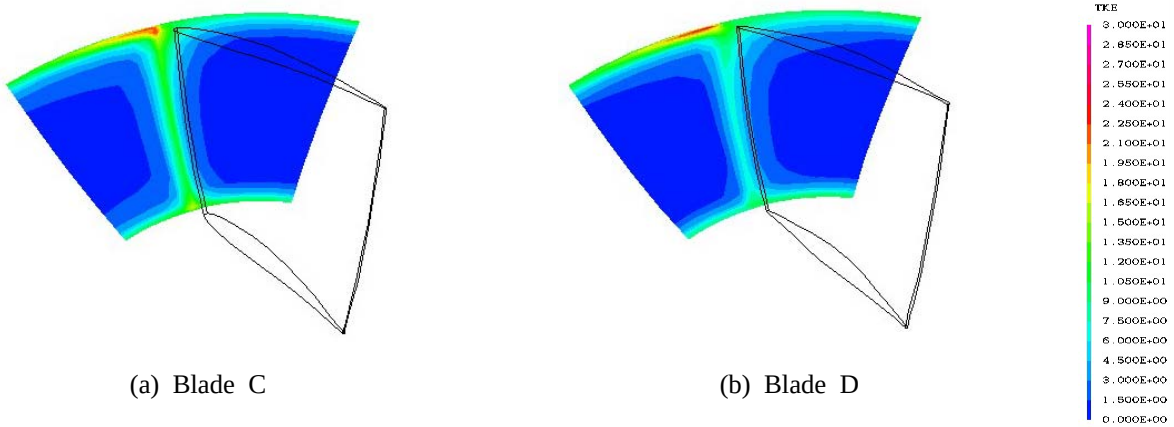

(a) Blade C (b) Blade D

Fig. 13 Contour map of turbulence kinetic energy at the exit of rear blade (θ = 0 deg, n = 2000 rpm)

5. Conclusions

To actualize the thin leading edge of blade, the wall profile consisting of convex and concave curves is considered, and its capability for bidirectional flow is studied by using a two-stage jet fan of JF600 class. From an experimental and numerical study, the following conclusions are drawn:

1. The proposed blade profile, called Blade D in this paper, is sufficiently usable for rotor blades of an advanced jet fan.
2. Improved fan performance indicates that not only the blade profile but the sweep effect of the secondary flow from the root to the tip along the blade surface almost assists the stable reattachment of separating flow on the rotating blades.
3. The performance of 2 stage jet fan and the internal flow are reasonably predicted by a turbulent flow analysis.

Acknowledgments

We would like to thank Fuji Electric Systems Co., Ltd. for their support. We also thank Mr. Hiroki Sunami and Mr. Shingo Shudou for their contributions to this work as their graduate studies.

Nomenclature

A_j	Ccross sectional area of cylindrical casing, = πR^2	SPL	sound pressure level [dB]
AR	aspect ratio	SPL_{SA}	specific noise level (A characteristic)
F	axial thrust [N]	U_t	tip speed of rotor blade [m/s]
L	shaft power [W]	V_u	circumferential component of velocity [m/s]
n	rotational speed [rpm]	V_z	axial component of velocity [m/s]
P	pressure [Pa]	η	fan total efficiency
P_t	total pressure [Pa]	θ	setting angle of blade
P_T	total pressure rise of fan [Pa]	ρ	density [kg/m^3]
Q	flow rate [m^3/s or m^3/min]	σ	solidity
R	radius of fan casing, = 0.315 m	Subscripts	
r	radial distance [m]	1,2,3,4,5,6	measurement section

References

[1] Abbot, I.H., and von Doenhoff, A.E., 1949, Theory of Wing Sections, Dover.

[2] Nishioka, T., Terasaka, H., and Kozu, T., 2000, “New Jet Fan for Tunnel Ventilation,” Turbomachinery, Vol. 28, No. 6, pp. 357-363 (in Japanese).

[3] Tukamoto, T., Niikura, Y., and Nishi, M., 1991, “Development of Jet Fans for Tunnel Ventilation,” Aerodynamics and Ventilation of Vehicle Tunnels, pp. 847-858, Elsevier.

[4] Nishi, M., Yoshida, K., Matsuda, I., Yamasaki, K., and Kojima, K., 2002, “Aerodynamic Performance of 2-Stage Jet Fan Having Forced-Vortex-Type Rotor,” Proceedings of 9th International Symposium on Transport Phenomena and Dynamics of Rotating Machinery, Honolulu.